Alexandria Engineering Journal (2014) 53, 737–745

Alexandria University

Alexandria Engineering Journal

www.elsevier.com/locate/aej
www.sciencedirect.com

ORIGINAL ARTICLE

Nanofluid flow over an unsteady stretching surface in presence of thermal radiation

Kalidas Das [a,*], Pinaki Ranjan Duari [b,1], Prabir Kumar Kundu [b,2]

[a] Dept. of Mathematics, Kalyani Govt. Engg. College, Kalyani 741235, W.B., India
[b] Dept. of Mathematics, Jadavpur University, Kolkata 700032, W.B., India

Received 27 December 2013; revised 28 April 2014; accepted 14 May 2014
Available online 14 June 2014

KEYWORDS

Nanofluid;
Heat and mass transfer;
Stretching sheet;
Thermal radiation

Abstract This paper investigates the unsteady boundary layer flow of a nanofluid over a heated stretching sheet with thermal radiation. The transport model employed includes the effects of Brownian motion and thermophoresis. The unsteadiness in the flow field is caused by the time-dependence of the stretching velocity, free stream velocity and the surface temperature. The unsteady boundary layer equations are transformed to a system of non-linear ordinary differential equations and solved numerically using a shooting method together with Runge–Kutta–Fehlberg scheme. The clear liquid results from this study are in agreement with the results reported in the literature. It is found that the heat transfer rate at the surface increases in the presence of Brownian motion but reverse effect occurs for thermophoresis.

1. Introduction

Stagnation point flow of an incompressible viscous fluid induced by a stretching sheet has important practical applications in many industries, such as the aerodynamics extrusion of plastic sheets, the cooling of metallic plate, continuous stretching of plastic films and artificial fibers. Extensive research on boundary layer flow over a stretching surface has been under taken since pioneering work of Sakiadis [1] because of its engineering applications. Crane [2] obtained a closed form solution for a stretching sheet whose velocity is proportional to the distance from the slit. Further, Weidman and Magyari [3], Chen and Char [4], Dutta et al. [5] etc. have studied various aspects of the problem of a stretching sheet in its own plane and of the stagnation point flow toward a stretching sheet. The studies mentioned above dealt with the steady flows, but many problems of practical interest may be unsteady. The unsteadiness is due to the change in the stretching velocity, free stream velocity or wall temperature etc. The mechanical and thermal characteristics of such an unsteady process were investigated both analytically and numerically in the boundary layer approximation, assuming a linear variation in the steady stretching velocity with the longitudinal

* Corresponding author. Tel.: +91 9748603199.
E-mail addresses: kd_kgec@rediffmail.com (K. Das), pinakiranjanduari@gmail.com (P.R. Duari), kunduprabir@yahoo.co.in (P.K. Kundu).
[1] Tel.: +91 8001873402.
[2] Tel.: +91 943315434.

Peer review under responsibility of Faculty of Engineering, Alexandria University.

Production and hosting by Elsevier

1110-0168 © 2014 Production and hosting by Elsevier B.V. on behalf of Faculty of Engineering, Alexandria University.
http://dx.doi.org/10.1016/j.aej.2014.05.002

coordinate and an inverse linear law for its decrease with time during the gradual switch-off process. Various aspects of the unsteady stretching sheet problem have been investigated by many authors (cf. [6–10]).

The effects of thermal radiation on the flow and heat transfer have important applications in physics and engineering, especially, in space technology and high temperature processes. Thermal radiation effects may also play an important role in controlling heat transfer in industry where the quality of the final product depends on the heat controlling factors to some extent. The effects of radiation on heat transfer problems have studied by Raptis [11], Makinde [12], Ibrahim et al. [13], Hayat et al. [14], Pal [15], Shit and Haldar [16]. Recently, Das [17] investigated the impact of thermal radiation on MHD slip flow over a flat plate with variable fluid properties.

Considerable efforts have been directed toward the study of the boundary layer flow and heat transfer over a stretching sheet because of its numerous industrial applications such as electronic, power, manufacturing, aerospace and transportation industries. Common heat transfer fluids such as water, ethylene glycol, toluene and engine oil have limited heat transfer capabilities due to their low heat transfer properties. In contrast, metals have higher thermal conductivities than these fluids. Therefore, it is desirable to combine the two substances to produce a heat transfer medium that behaves like a fluid but has the higher heat transfer properties. The term nanofluid refers to a liquid suspension containing tiny particles having diameter less than 50 nm. Choi [18] experimentally verified that addition of small amount of nanoparticles appreciably enhances the effective thermal conductivity of the base fluid. The common nanoparticles that have been used are aluminum, copper, iron and titanium or their oxides. Various benefits of the application of nanofluids include the following: improved heat transfer, heat transfer system size reduction, micro-channel cooling and miniaturization of the system. A comprehensive survey of convective transport in nanofluids was made by Buongiorno [19] who considered seven slip mechanisms that can produce a relative velocity between nanoparticles and the base fluid. Of all these mechanisms, only Brownian diffusion and thermophoresis were found to be important. An excellent assessment of nanofluid physics and developments has been provided by Das et al. [20] and Eastman et al. [21]. The influences of nanoparticles on natural convection boundary layer flow past a vertical plate by taking Brownian motion and thermophoresis into account was investigated by Kuznetsov and Nield [22]. Godson et al. [23] presented an overview on experimental and theoretical studies on convective heat transfer in nanofluids and their applications.

Akyildiz et al. [24] discussed nanoboundary layer fluid flows over stretching surfaces. Chamkha et al. [25] investigated the mixed convection flow of a nanofluid past a stretching surface in the presence of Brownian motion and thermophoresis effects. Das [26] studied Lie group analysis of stagnation-point flow of a nanofluid. Nanofluid flow over a shrinking sheet in the presence of surface slip was discussed by Das [27]. Recently heat transfer analysis of nanofluid over an exponentially stretching sheet was investigated by Nadeem et al. [28].

The objective of the present work was to study the effect of thermal radiation on boundary layer flow of a nanofluid over a heated stretching sheet with an unsteady free stream condition. Numerical results are obtained using a shooting technique together with Runge–Kutta–Fehlberg schemes. The paper is organized as follows. Mathematical analysis regarding problem formulation is presented in Section 2. Section 3 comprises the method of solution and code verification. Discussion related to plots is presented in Section 4. Section 5 lists the main observations.

2. Mathematical analysis

2.1. Governing equations

Considering the two-dimensional unsteady boundary layer flow of a nanofluid over a heated stretching sheet with thermal radiation, the coordinate system under consideration is such that x measures the distance along the sheet and y measures the distance normally into the fluid (Fig. 1). The flow is assumed to be confined to $y > 0$. Two equal and opposite forces are impulsively applied along the x-axis so that the sheet is stretched keeping to fixed origin. Let us consider that for time $t < 0$ the fluid and heat flows are steady. The unsteady fluid and heat flows start at $t = 0$, the sheet being stretched with the velocity $U_w(x, t)$ along the x-axis. It is also assumed that the ambient fluid is moved with a velocity $U_e(x, t)$ in the y-direction toward the stagnation point on the plate. The temperature of the sheet $T_w(x, t)$ and the value of nanoparticle volume fraction $C_w(x, t)$ at the surface vary both with the distance x along the sheet and time t and higher than the ambient temperature T_∞ and concentration C_∞ respectively. In view of thermal equilibrium, there is no slip between the base fluid and suspended nanoparticles. Since the velocity of the nanofluid is low (laminar flow), the viscous dissipative heat is assumed to be negligible here.

Under the above assumptions, the basic unsteady conservation of mass, momentum, thermal energy equations of nanofluid and nanoparticle fraction in the presence of thermal radiation past a stretching sheet can be expressed as follows (see Refs. [6,8,26]):

$$\frac{\partial u}{\partial x}+\frac{\partial v}{\partial y}=0 \tag{1}$$

$$\frac{\partial u}{\partial t}+u\frac{\partial u}{\partial x}+v\frac{\partial u}{\partial y}=\frac{\partial U_e}{\partial t}+U_e\frac{\partial U_e}{\partial x}+\nu_f\frac{\partial^2 u}{\partial y^2} \tag{2}$$

$$\frac{\partial T}{\partial t}+u\frac{\partial T}{\partial x}+v\frac{\partial T}{\partial y}=\alpha\frac{\partial^2 T}{\partial y^2}+\tau\left[D_B\frac{\partial C}{\partial y}\frac{\partial T}{\partial y}+\left(\frac{D_T}{T_\infty}\right)\left(\frac{\partial T}{\partial y}\right)^2\right]-\frac{1}{(\rho c)_f}\frac{\partial q_r}{\partial y} \tag{3}$$

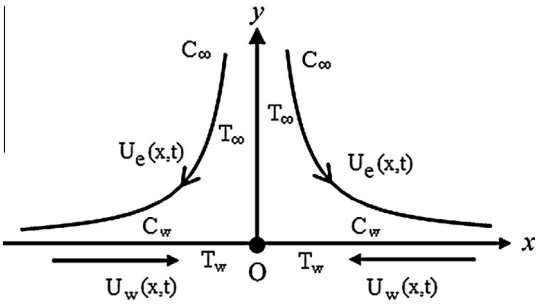

Figure 1 Physical model and coordinate system.

$$\frac{\partial C}{\partial t}+u\frac{\partial C}{\partial x}+v\frac{\partial C}{\partial y}=D_B\frac{\partial^2 C}{\partial y^2}+\left(\frac{D_T}{T_\infty}\right)\frac{\partial^2 T}{\partial y^2} \tag{4}$$

where u, v are the velocity components along the x and y directions respectively, ρ_f is the density of the base fluid, μ_f is the kinematic viscosity of the base fluid (water), $\alpha=\frac{\kappa}{(\rho c)_f}$ is the thermal diffusivity of the base fluid, $\tau=\frac{(\rho c)_s}{(\rho c)_f}$ is the ratio of the nanoparticle heat capacity and the base fluid heat capacity, $(\rho c)_f$ and $(\rho c)_s$ are the specific heat parameters of the base fluid and nanoparticle, respectively, T is temperature of the fluid, C is the nanoparticle volume fraction, T_∞ and C_∞ are the temperature and the nanoparticle fraction of the fluid far from the sheet, D_B is the Brownian diffusion coefficient, D_T is the thermophoretic diffusion coefficients and q_r is the radiative heat flux in the y-direction.

Using the Rosseland approximation, the radiative heat flux is given by (cf. Brewster [29])

$$q_r=-\frac{4\sigma^*}{3k^*}\frac{\partial T^4}{\partial y} \tag{5}$$

where σ^* is the Stefan–Boltzmann constant and k^* is the mean absorption coefficient. Assuming that the differences in temperature within the flow are such that T^4 can be expressed as a linear combination of the temperature, T^4 may be expanded in Taylor's series about T_∞ and neglecting higher order terms, one may get

$$T^4=4T_\infty^3T-3T_\infty^4 \tag{6}$$

Thus

$$\frac{\partial q_r}{\partial y}=-\frac{16T_\infty^3\sigma^*}{3k^*}\frac{\partial^2 T}{\partial y^2} \tag{7}$$

Using Eq. (7), the energy Eq. (3) becomes

$$\frac{\partial T}{\partial t}+u\frac{\partial T}{\partial x}+v\frac{\partial T}{\partial y}=\alpha\left(1+\frac{16T_\infty^3\sigma^*}{3k^*\kappa}\right)\frac{\partial^2 T}{\partial y^2}+\tau\left[D_B\frac{\partial C}{\partial y}\frac{\partial T}{\partial y}+\left(\frac{D_T}{T_\infty}\right)\left(\frac{\partial T}{\partial y}\right)^2\right] \tag{8}$$

2.2. Boundary conditions

The appropriate boundary conditions for the problem are as follows:

$$\left.\begin{aligned}&u=U_w(x,t),v=0,T=T_w(x,t),C=C_w(x,t)\quad\text{at}\quad y=0\\&u\to U_e(x,t),T\to T_\infty,C\to C_\infty\quad\text{as}\quad y\to\infty\end{aligned}\right\} \tag{9}$$

Here the stretching velocity $U_w(x, t)$ is of the form

$$U_w=\frac{ax}{1-\lambda t} \tag{10}$$

where a (stretching rate) and λ are positive constants having dimension $(time)^{-1}$ (with $\lambda t<1,\lambda\geq 0$). It is noted that the stretching rate $\frac{a}{1-\lambda t}$ increases with time since $a>0$. The free stream velocity is of the form

$$U_e=\frac{bx}{1-\lambda t} \tag{11}$$

where b (>0) is the strength of the stagnation flow. The wall temperature $T_w(x, t)$ and the value of nanoparticle volume fraction $C_w(x, t)$ are given by

$$T_w(x,t)=T_\infty+T_0\left[\frac{ax^2}{2\nu_f}\right](1-\lambda t)^{-2} \tag{12}$$

$$C_w(x,t)=C_\infty+C_0\left[\frac{ax^2}{2\nu_f}\right](1-\lambda t)^{-2} \tag{13}$$

where T_∞ and C_∞ are the free stream values of temperature and nanoparticle volume fraction respectively and T_0 and C_0 are positive reference temperature and nanoparticle volume fraction respectively such that $0\leqslant T_0\leqslant T_w$ and $0\leqslant C_0\leqslant C_w$. Note that the above expressions are valid for time $t<\lambda^{-1}$ and are chosen in order to devise a similarity transformation which transform the governing partial differential equations into a set of highly nonlinear ordinary differential equations.

2.3. Non-dimensionalization

The governing equations and boundary conditions are simplified by introducing the following dimensionless functions f, θ and φ, and the similarity variable η:

$$\left.\begin{aligned}&\eta=\sqrt{\tfrac{a}{\nu_f(1-\lambda t)}}y,\psi=\sqrt{\tfrac{a\nu_f}{(1-\lambda t)}}xf(\eta),\\&T=T_\infty+T_0\left[\tfrac{ax^2}{(1-\lambda t)^{-2}}\right]\theta(\eta),C=C_\infty+C_0\left[\tfrac{ax^2}{(1-\lambda t)^{-2}}\right]\phi(\eta)\end{aligned}\right\} \tag{14}$$

where the stream function ψ is defined in the usual way as $u=\frac{\partial\psi}{\partial y}$ and $v=-\frac{\partial\psi}{\partial x}$. Thus from Eq. (1), we have

$$\left.\begin{aligned}&u=\left(\frac{ax}{1-\lambda t}\right)f'(\eta),\quad v=-\sqrt{\frac{a\nu_f}{1-\lambda t}}f(\eta)\end{aligned}\right\} \tag{15}$$

where primes denote differentiation with respect to η.

Now substituting Eq. (14) into Eqs. (2), (4), (8), the following ordinary differential equations are obtained as follows:

$$f'''+f''\left(f-\frac{1}{2}\eta S\right)-f'(f'+S)+\beta^2+\beta S=0 \tag{16}$$

$$\frac{1}{\mathrm{Pr}}(1+Nr)\theta''-S\left(2\theta+\frac{1}{2}\eta\theta'\right)+f\theta'-2f'\theta+Nb\theta'\phi'+Nt\theta'^2=0 \tag{17}$$

$$\frac{1}{Le}\phi''-S\left(2\phi+\frac{1}{2}\eta\phi'\right)+f\phi'-2f'\phi+\frac{Nt}{LeNb}\theta''=0 \tag{18}$$

The boundary conditions (9) take the form

$$\left.\begin{aligned}&f'(0)=1,f(0)=0,\theta(0)=1,\phi(0)=1,\\&f'(\infty)=\beta,\theta(\infty)=0,\phi(\infty)=0\end{aligned}\right\} \tag{19}$$

where $S=\frac{\lambda}{a}$ is the unsteadiness parameter, $\beta=\frac{b}{a}$ is the stretching parameter, $\mathrm{Pr}=\frac{\nu_f}{\alpha}$ is the Prandtl number, $Nr=\frac{16T_\infty^3\sigma^*}{3k^*\kappa}$ is the thermal radiation parameter, $Nb=\frac{\tau D_B(C_w-C_\infty)}{\nu_f}$ is the Brownian motion number, $Nt=\frac{\tau D_T(T_w-T_\infty)}{\nu_f T_\infty}$ is the thermophoresis number, $Le=\frac{\nu_f}{D_B}$ is the Lewis number.

2.4. Physical quantities of engineering interest

The quantities of physical interest in this problem are the skin friction coefficient C_f, the local Nusselt number Nu and the local Sherwood number Sh which are defined as follows:

$$C_f = \frac{\mu}{\rho_f U_w^2}\left(\frac{\partial u}{\partial y}\right)_{y=0} \tag{20}$$

$$Nu = \frac{x}{\kappa(T_w - T_\infty)}\left[\kappa\left(\frac{\partial T}{\partial y}\right)_{y=0} - \frac{4\sigma^*}{3k^*}\left(\frac{\partial T^4}{\partial y}\right)_{y=0}\right] \tag{21}$$

$$Sh = -\frac{x}{(C_w - C_\infty)}\left(\frac{\partial C}{\partial y}\right)_{y=0} \tag{22}$$

Substituting Eq. (14) into (20), (22), one may obtain

$$C_f r = \mathrm{Re}_x^{\frac{1}{2}} C_f = f''(0) \tag{23}$$

$$Nur = \mathrm{Re}_x^{\frac{1}{2}} Nu = -(1 + Nr)\theta'(0) \tag{24}$$

$$Shr = \mathrm{Re}_x^{\frac{1}{2}} Sh = -\phi'(0) \tag{25}$$

where $C_f r$ is the reduced skin friction coefficient, Nur is the reduced Nusselt number and Shr is the reduced Sherwood number and $\mathrm{Re}_x = \frac{U_w x}{\nu_f}$ is the local Reynolds number based on the sheet velocity U_w.

2.5. Particular case

The present problem reduces to steady-state flow for $S = 0$. In the absence of diffusion equation, Brownian motion, thermophoresis and thermal radiation, Eqs. (16)–(18) and the boundary conditions (19) reduce to Eqs. (6), (7) and the boundary conditions (8) of Ishak et al. [8] by setting $\lambda = 0$ of their paper. Thus, in the absence of buoyancy force and stretching parameter (i.e., $\lambda = \beta = 0$), the Eqs. (6), (7) and the boundary conditions (8) of Ishak et al. [8] reduces to

$$f''' + ff'' - f'^2 = 0 \tag{26}$$

$$\frac{1}{\mathrm{Pr}}\theta'' + f\theta' - 2f'\theta = 0 \tag{27}$$

and

$$\left.\begin{aligned} f'(0) = 1, f(0) = 0, \theta(0) = 1, \\ f'(\infty) = 0, \theta(\infty) = 0 \end{aligned}\right\} \tag{28}$$

The closed-form solution of the above Eq. (26) subject to the boundary conditions (28) is

$$f(\eta) = 1 - e^{-n} \tag{29}$$

which is the Crane's solution for a stretching sheet problem (see Crane [2]). Again using Eq. (29), the solution of the Eq. (27) subject to the boundary conditions (28) in terms of confluent hypergeometric functions is given by (Ishak et al. [8])

$$\theta(\eta) = \frac{M(\mathrm{Pr} - 2, \mathrm{Pr} + 1, -Pre^{-n})}{M(\mathrm{Pr} - 2, \mathrm{Pr} + 1, -\mathrm{Pr})} \tag{30}$$

where $M(a, b, z)$ denotes the confluent hypergeometric function as follows

$$M(a, b, z) = 1 + \sum_{n=1}^{\infty} \frac{a_n}{b_n}\frac{z^n}{n!}$$

where $a_n = a(a+1)(a+2)\ldots(a+n-1)$,
$b_n = b(b+1)(b+2)\ldots(b+n-1)$.

Using Eqs. (29) and (30), the skin friction coefficient $f''(0)$ and local Nusselt $-\theta'(0)$ are given by

$$f''(0) = -1 \tag{31}$$

$$\theta'(0) = \mathrm{Pr}\left\{\frac{\mathrm{Pr} - 2}{\mathrm{Pr} + 1}\frac{M(\mathrm{Pr} - 1, \mathrm{Pr} + 2, -Pre^{-n})}{M(\mathrm{Pr} - 2, \mathrm{Pr} + 1, -\mathrm{Pr})} - 1\right\} \tag{32}$$

3. Method of solution

The set of non-linear coupled differential Eqs. (16)–(18) with appropriate boundary conditions given in Eq. (19) constitute a two-point boundary value problem. The equations are highly non-linear and so, cannot be solved analytically. Therefore, these equations are solved numerically using the symbolic computer algebra software Maple 17. This software uses a Runge–Kutta–Fehlberg method as the default to solve the boundary value problems numerically. The asymptotic boundary conditions in (19) at $\eta \to \infty$ are replaced by those at $\eta = \eta_\infty$ as is usually the standard practice in the boundary layer analysis. The inner iteration is counted until the nonlinear solution converges with a convergence criterion of 10^{-6} in all cases.

3.1. Testing of the code

To check the validity of the present code, the values of $f''(0)$ have been calculated for different values of stretching ratio parameter β for the case of steady flow (i.e., for $S = 0$) of Newtonian fluid (i.e., Nb = Nt = 0) and in the absence of thermal radiation parameter (i.e., Nr = 0) in Table 1. From table, it has been observed that the data produced by the Maple code and those reported by Ishak et al. [8], Mahapatra and Gupta [6] are in excellent agreement and, so this gives us confidence to use the present code. The profiles of fluid velocity versus boundary layer coordinate have been plotted in Fig. 2 for various values of β in the absence of mass transfer. It is observed that the results agree very well with those of Mahapatra and Gupta [6].

4. Results and discussion

In order to analyze the results, numerical computation has been carried out (using the method described in the previous section), for various values of the unsteadiness parameter S, thermophoretic parameter Nt, Brownian motion parameter Nb, and Lewis number Le. In the simulation the default values of the parameters are considered as $S = 0.4$, Nb = 0.1, Nt = 0.1, Pr = 0.71, Nr = 0.2 and $\beta = 0.5$ unless otherwise specified.

Table 1 Comparison of the values of $f''(0)$ for various values of β.

β	Mahapatra and Gupta [6]	Ishak et al. [8]	Present work
	f'(0)		
0.1	−0.9694	−0.9694	−0.969328
0.2	−0.9181	−0.9181	−0.918098
0.5	−0.6673	−0.6673	−0.667301
2.0	2.0175	2.0175	2.017467
3.0	4.7293	4.7294	4.729406

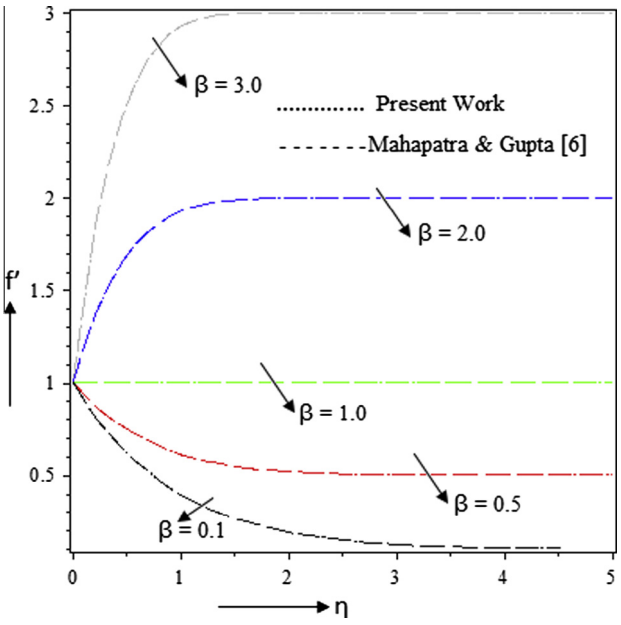

Figure 2 Velocity profiles in the absence of mass transfer.

4.1. Effect of thermal radiation parameter Nr

Fig. 3 illustrates the changes that are seen in temperature profiles due to increase in the values of thermal radiation parameter Nr for the case of steady flow ($S = 0$) and unsteady flow ($S = 0.4$). It is observed that the fluid temperature increases as Nr increases due to the fact that the conduction effect of the nanofluid increases in the presence of thermal radiation. Therefore higher values of radiation parameter imply higher surface heat flux and so, increase the temperature within the boundary layer region. It is also observed that thermal boundary layer thickness increases with increasing the values of Nr for both steady and unsteady cases. The impact of thermal radiation parameter Nr on the nanoparticles volume fraction profiles is presented in Fig. 4. It can easily be seen from figure that the nanoparticle volume fraction decreases near the boundary surface i.e. for $\eta < 1.2$ (not precisely determined) but effect is reverse for $\eta > 1.2$ (not precisely determined). From Table 2 one may see that Nr enhances the rate of heat transfer whereas it reduces the rate of mass transfer at the stretching surface. It should be noted that the effect is prominent for unsteady flow than that of steady flow.

4.2. Effect of Lewis number Le

Fig. 5 demonstrates the influence of Lewis number Le on temperature distribution within the boundary layer in the presence of thermal radiation, Brownian motion and thermophoresis. It is observed from the figure that the temperature profiles as well as the thickness of the thermal boundary layer increase with increase in the values of Lewis number Le for both steady and unsteady flows but effect is not significant. Fig. 6 exhibits the nanoparticle volume fraction profiles for several values of Lewis number Le for both steady and unsteady flows. It is seen that the nanoparticle volume fraction decreases with the increase in Le and this implies an accompanying reduction in the thickness of the concentration boundary layer thickness. Also the nanoparticle volume fraction profiles decrease asymptotically to zero at the edge of the boundary layer. It is evident from Table 2 that the Nusselt number Nur increases on increasing Le but the effect is reverse on the Sherwood number Shr.

4.3. Effect of Brownian motion parameter Nb

The variation in the dimensionless temperature with η is shown in Fig. 7 for some values of Brownian motion parameter Nb

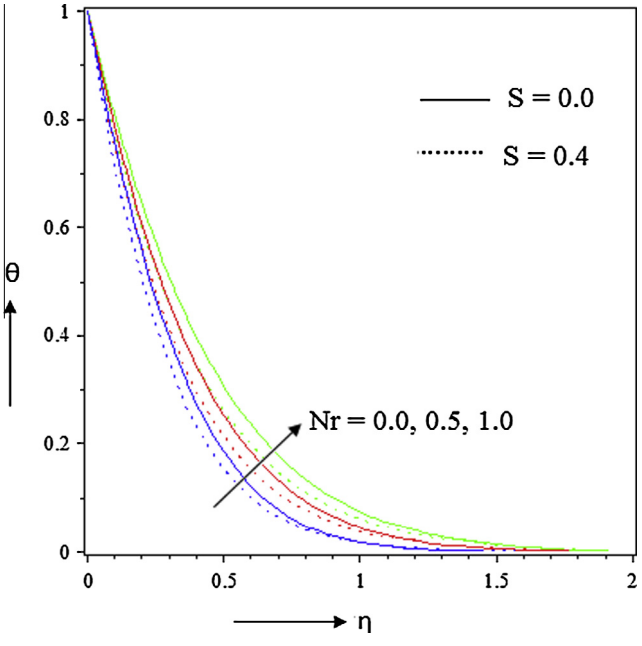

Figure 3 Temperature profiles for various values of Nr.

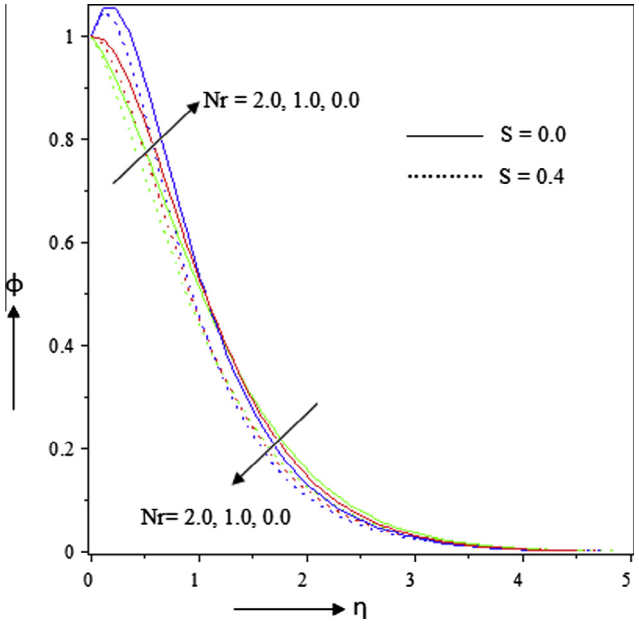

Figure 4 Nanoparticle concentration profiles for various values of Nr.

Table 2 Effects of Le, Nr, Nb and Nt on Nur and Shr.

Le	Nr	Nb	Nt	Nur		Shr	
				S = 0.0	S = 0.	S = 0.0	S = 0.4
1	0.1	0.1	0.1	−0.42520681	−0.42008811	2.69127557	3.09206857
5				2.39823855	2.72467142	2.39487484	2.72467142
10				4.22940342	4.773802290	2.27100139	2.63888824
5	0.0			2.21498396	2.51677464	2.66697226	3.09287098
	0.5			2.42081168	2.75830626	2.33210820	2.70652145
	1.0			2.563140865	2.92250981	2.093332374	2.43363675
	0.4	0.1		−0.42520681	−0.41911007	2.69127557	2.99634364
		0.3		0.93222493	1.06572445	2.26135139	2.52948256
		0.6		1.24904151	1.41250660	1.75382678	1.97846755
		0.1	0.1	−0.42520681	−0.42008811	2.69127557	3.09206857
			0.3	−3.29753099	−3.64608553	2.384952118	2.745157612
			0.5	−5.35791536	−5.95222114	2.13476075	2.46200249

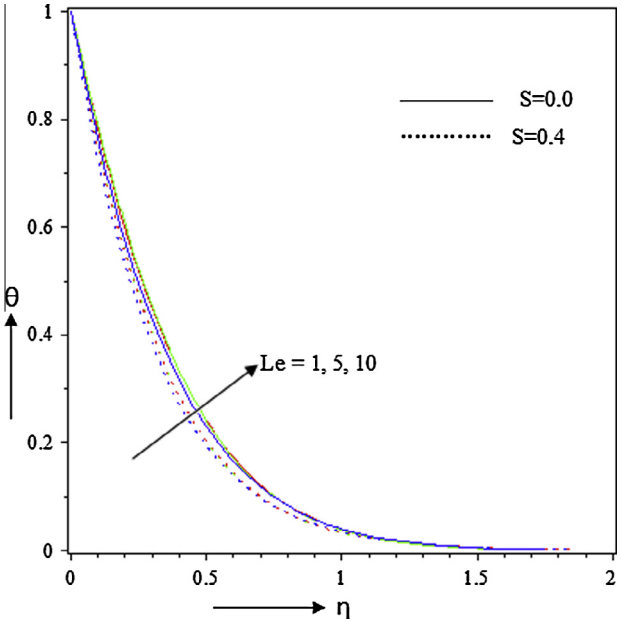

Figure 5 Temperature profiles for various values of Le.

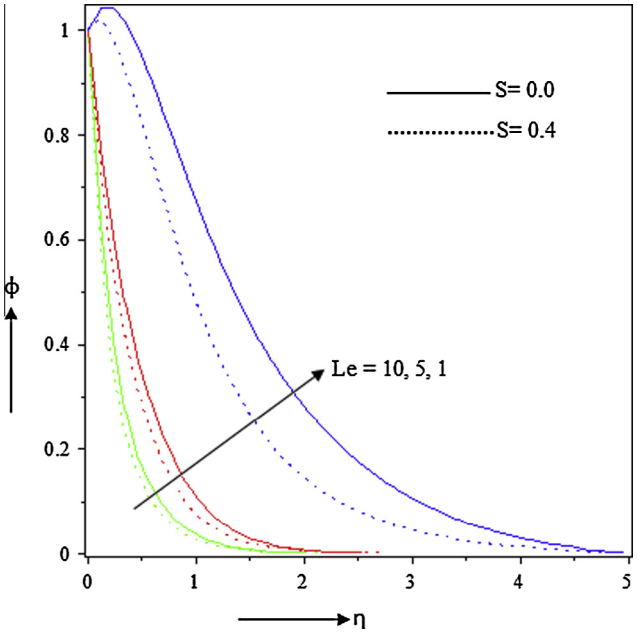

Figure 6 Nanoparticle concentration profiles for various values of Le.

when $S = 0$, 0.4. The results in the figure show that the fluid temperature is found to increase with the increase in Nb for both $S = 0$ and $S = 0.4$. The physics behind this phenomenon is that the increased Brownian motion increases the thickness of thermal boundary layer, which ultimately enhances the temperature. The nanoparticle volume fraction distribution is presented in Fig. 8 for various values of Brownian motion parameter Nb when $S = 0.0$ (for steady flow), 0.4 (for unsteady flow). The curves show that the nanoparticle volume fraction decreases with increasing Nb near the boundary layer region for both steady and unsteady flows. From Table 2 one can see that the effect of Nb is to increase the Nusselt number at the surface of the plate whereas the effect is opposite on Sherwood number.

4.4. Effect of thermophoretic parameter Nt

The effect of thermophoretic parameter Nt is same as for Brownian motion parameter Nb as one can see from Fig. 9. Thus fluid temperature increases on increasing Nb in the boundary layer region and, as a consequence, thickness of the thermal boundary layer increases. This enhancement is due to the nanoparticle of high thermal conductivity being driven away from the hot sheet to the quiescent nanofluid. It is seen from Fig. 10 that the thermophoretic parameter Nt produces an increase in the nanoparticle volume fraction for both the steady and unsteady cases. It is interesting to note from the figure that distinctive peaks in the profiles occur in region adjacent to the wall for higher values of thermophoretic parameter Nt. This means that the nanoparticle volume fraction near the sheet is higher than the nanoparticle volume fraction at the sheet and consequently, and nanoparticles are expected to transfer to the sheet due to the thermophoretic effect. The Nusselt number Nur and Sherwood number both decrease on increasing thermophoretic parameter Nt as presented in Table 2.

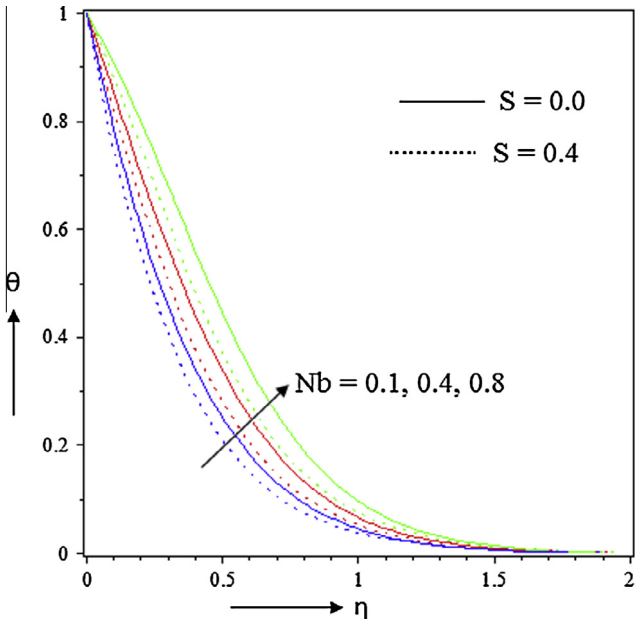

Figure 7 Temperature profiles for various values of Nb.

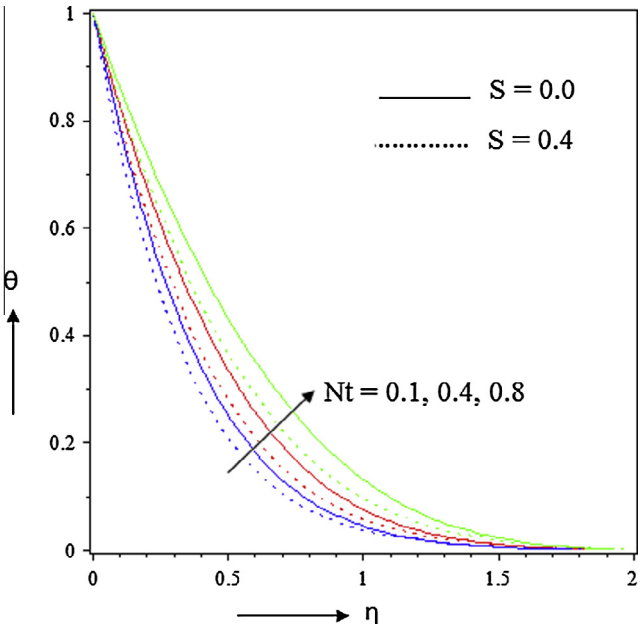

Figure 9 Temperature profiles for various values of Nt.

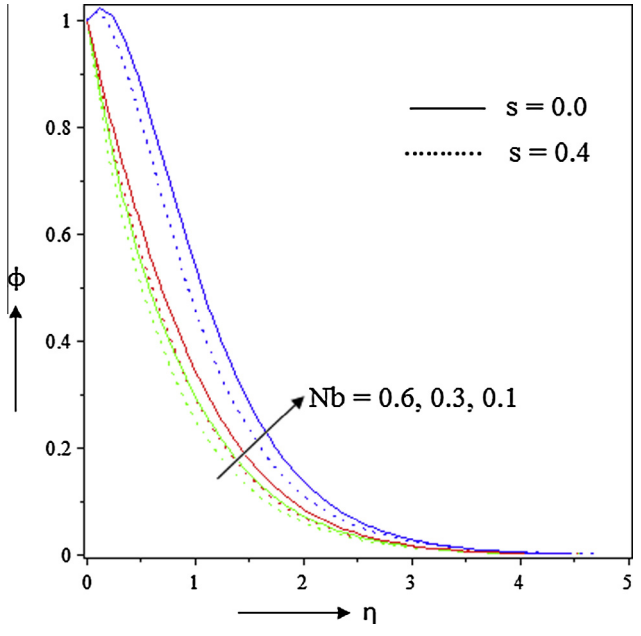

Figure 8 Nanoparticle concentration profiles for various values of Nb.

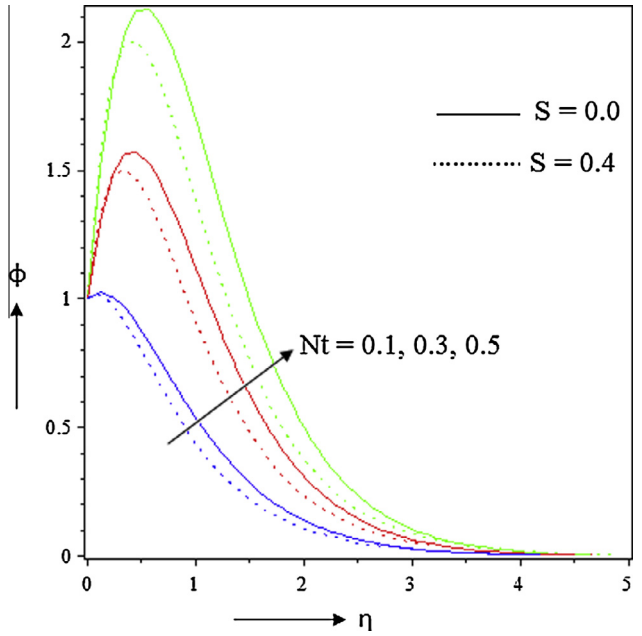

Figure 10 Nanoparticle concentration profiles for various values of Nt.

4.5. Effect of unsteadiness parameter S

The effects of the unsteadiness parameter S on temperature profiles are depicted in Fig. 11. It is observed from the figure that as S increases the profiles of temperature decreases with a marked decrease in boundary layer thickness. It is note worthy that temperature profiles satisfy the far field boundary conditions asymptotically, thus supporting the validity of the numerical results obtained. Plots of the nanoparticle volume fraction for different values of unsteadiness parameter S are shown in Fig. 12. It is noticed from the figure that the nanoparticle volume fraction decreases with increase in the values of S near the boundary layer region in the presence of thermal radiation and satisfies the far field boundary conditions asymptotically. Thus, by escalating S, concentration boundary layer thickness decreases. One may note that the effect of S is more effective for regular fluid (water) than nanofluid. Table 3 shows that the rate of heat transfer and rate of mass transfer both increase on increasing unsteadiness parameter S and the effect is prominent for nanofluid than that for regular fluid.

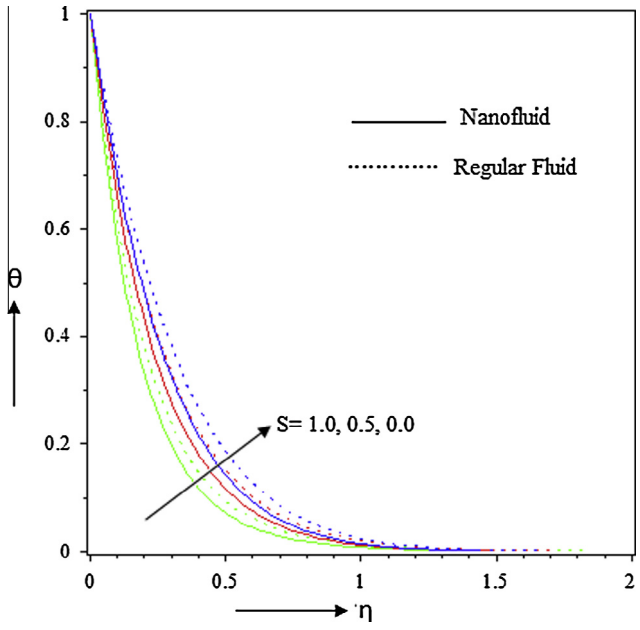

Figure 11 Temperature profiles for various values of *S*.

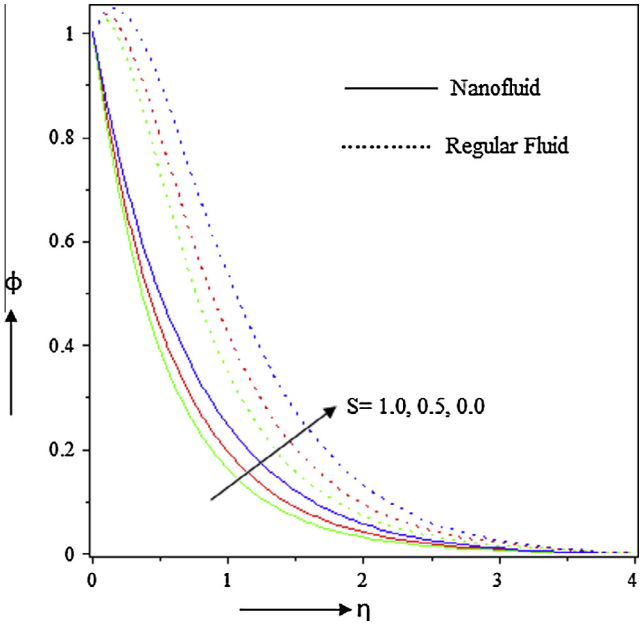

Figure 12 Nanoparticle concentration profiles for various values of *S*.

5. Final remarks

In this work, the effect of thermal radiation on boundary layer flow of a nanofluid over a heated stretching sheet with an unsteady free stream condition is investigated numerically. The governing equations are transformed into non-linear ordinary differential equations using similarity transformations and then solved numerically by employing a shooting technique together with Runge–Kutta–Fehlberg schemes. A parametric study is performed to explore the effects of various governing parameters on heat and mass transfer characteristics.

Table 3 Effects of *S* on Nur and Shr.

S	Nur		Shr	
	Nanofluid	Regular fluid	Nanofluid	Regular fluid
0.0	1.41745114	−0.68394393	3.56339618	2.98709551
0.5	1.70671502	−0.72217879	4.19078831	3.52682788
1.0	1.95102529	−0.77786271	4.74129519	4.00066640

Following conclusion can be drawn from the present investigation:

- Increasing the Brownian motion parameter, Lewis number and unsteadiness parameter lead to reduce the nanoparticle volume fraction near the boundary layer region but the effect is reverse for the thermophoretic parameter.
- The fluid temperature and the thermal boundary layer thickness increase for increasing thermal radiation, Brownian motion and thermophoresis whereas the effect is opposite for unsteadiness parameter.
- It is seen that the reduced Nusselt number increases while the reduced Sherwood number decreases as the Brownian motion parameter, Lewis number and thermal radiation parameter increase.
- A rise in the thermophoretic parameter reduces both the rate of heat transfer and the rate of mass transfer at the stretching surface.
- Moreover, it is observed that increase in the unsteadiness parameter enhances the reduced Nusselt number whereas the opposite trend is noticed in the case of the reduced Sherwood number.

Acknowledgements

Research was supported from, UGC, Government of India under the scheme of UGC-BSR research fellowship in science for meritorious students, gratefully acknowledged by second author. The authors wish to express their very sincere thanks to the reviewers for their valuable suggestions and comments to improve the presentation of this article.

References

[1] B.C. Sakiadis, Boundary layer behaviour on continus solid surface, AIChE J. 7 (1961) 6–28.
[2] L.J. Crane, Flow past a stretching plate, Z. Angew. Maths. Phys. 55 (1977) 744–746.
[3] P.D. Weidman, E. Magyari, Generalised Crane flow induced by continuous surfaces stretching with arbitrary velocities, Acta Mechanica 209 (2009) 353–362.
[4] C.K. Chen, M.I. Char, Heat transfer of a continuous stretching surface with suction or blowing, J. Math. Anal. Appl. 135 (1988) 568–580.
[5] B.K. Dutta, P. Roy, A.S. Gupta, Temperature field in flow over a stretching sheet with uniform heat flux, Int. Comm. Heat Mass Transfer 12 (1985) 89–94.
[6] T.R. Mahapatra, A.S. Gupta, Heat transfer in stagnation-point flow towards a stretching sheet, Heat Mass Transfer 38 (2002) 517–521.
[7] E.M.A. Elbashbeshy, M.A.A. Bazid, Heat transfer over an unsteady stretching isothermal stretching sheet immersed in a porous medium, Int. Comm. Heat Mass Transfer 41 (2004) 1–4.

[8] A. Ishak, R. Nazar, I. Pop, Mixed convection boundary layer in the stagnation-point flow toward a stretching vertical sheet, Meccanica 41 (2006) 509–518.
[9] Abd. El-Aziz, A Flow and heat transfer over an unsteady stretching surface with Hall effect, Meccanica 45 (2010) 97–109.
[10] A.M. Rohni, S. Ahmadm, I. Pop, J.H. Merkin, Unsteady mixed convection boundary-layer flow with suction and temperature slip effects near the stagnation point on a vertical permeable surface embedded in a porous medium, Transp. Porous Med. 92 (1) (2012) 1–14.
[11] A. Raptis, Radiation and free convection flow through a porous medium, Int. Commun. Heat Mass Transfer 25 (1998) 289–295.
[12] D. Makinde, Free convection flow with thermal radiation and mass transfer past a moving vertical porous plate, Int. Commun. Heat Mass Transfer 32 (2005) 1411–1419.
[13] F.S. Ibrahim, A.M. Elaiw, A.A. Bakr, Influence of viscous dissipation and radiation on unsteady MHD mixed convection flow of micropolar fluids, Appl. Mathematics Inform. Sci. 2 (2008) 143–162.
[14] T. Hayat, Z. Abbas, I. Pop, S. Asghar, Effects of radiation and magnetic field on the mixed convection stagnation-point flow over a vertical stretching sheet in a porous medium, Int. J. Heat Mass Transfer 53 (2010) 466–476.
[15] D. Pal, Combined effects of non-uniform heat source/sink and thermal radiation on heat transfer over an unsteady stretching permeable surface, Commun. Nonlinear Sci. Numer. Simulat. 16 (2011) 1890–1904.
[16] G.C. Shit, R. Haldar, Effects of thermal radiation on MHD viscous fluid flow and heat transfer over nonlinear shrinking porous sheet, Appl. Mathematics Mech. (English Edition) 32 (6) (2011) 677–688.
[17] K. Das, Impact of thermal radiation on MHD slip flow over a flate plate with variable fluid properties, Heat Mass Transfer 48 (2012) 767–778.
[18] S.U.S. Choi, Enhancing thermal conductivity of fluids with nanoparticles, ASME Fluids Eng. Div. 231 (1995) 99–105.
[19] J. Buongiorno, Convective transport in nanofluids, ASME J. Heat Trans. 128 (2006) 240–250.
[20] S.K. Das, S. Choi, W. Yu, T. Pradeep, Nanofluids: Science and Technology, Wiley Interscience, New Jersey, 2007.
[21] J.A. Eastman, S.U.S. Choi, W. Yu, L.J. Thompson, Anomalously increased effective thermal conductivities of ethylene glycol-based nanofluids containing copper nanoparticles, Appl. Phys. Lett. 78 (2001) 718–720.
[22] A.V. Kuznetsov, D.A. Nield, Natural convection boundary-layer of a nanofluid past a vertical plate, Int. J. Them. Sci. 49 (2010) 237–243.
[23] L.B. Godson, D. Raja, D. Mohan Lal, S. Wongwisesc, Enhancement of heat transfer using nanofluids- an overview, Renew Sustain Energy Rev. 14 (2010) 629–641.
[24] F.T. Akyildiz, H. Bellout, K. Vajravelu, R.A. Van Gorder, Existence results for third order nonlinear boundary value problems arising in nano boundary layer fluid flows over stretching surfaces, Nonlinear Anal.: Real World Appl. 12 (2011) 2919–2930.
[25] A.J. Chamkha, R.S.R. Gorla, K. Ghodeswar, Non-similar solution for natural convective boundary layer flow over a sphere embedded in a porous medium saturated with a nanofluid, Transp. Porous Media 86 (2011) 13–22.
[26] K. Das, Lie group analysis of stagnation-point flow of a nanofluid, Microfluidics Nanofluidics 15 (2013) 267–274.
[27] K. Das, Nanofluid flow over a shrinking sheet with surface slip, Microfluidics Nanofluidics 16 (2014) 391–401.
[28] S. Nadeem, R.U. Haq, Z.H. Khan, Heat transfer analysis of water-based nanofluid over an exponentially stretching sheet, Alexandria Eng. J. 53 (1) (2014) 219–224.
[29] M.Q. Brewster, Thermal Radiative Transfer Properties, Wiley, New York, 1972.